Characterization of the 2-[(*R*)-2-Hydroxypropylthio]ethanesulfonate Dehydrogenase from *Xanthobacter* Strain Py2: Product Inhibition, pH Dependence of Kinetic Parameters, Site-Directed Mutagenesis, Rapid Equilibrium Inhibition, and Chemical Modification[†]

Daniel D. Clark and Scott A. Ensign*

Department of Chemistry and Biochemistry, Utah State University, Logan, Utah 84322-0300

Received September 17, 2001; Revised Manuscript Received December 13, 2001

ABSTRACT: Although the short-chain dehydrogenase/reductase (SDR) superfamily contains a very large number of members defined in annotated databases and by biochemical and structural studies, very few SDR enzymes have been identified that have a homologous partner catalyzing the same reaction but with an opposite stereospecificity. In the present study we have cloned and expressed one of these enzymes, the 2-[(*R*)-2-hydroxypropylthio]ethanesulfonate (R-HPC) dehydrogenase, that is part of the coenzyme M-dependent pathway of alkene and epoxide metabolism in *Xanthobacter* strain Py2. Investigation of the kinetic mechanism using product inhibition suggested that a compulsory-ordered ternary complex mechanism was followed. The pH dependence of k_{cat}/K_m indicated the presence of a single ionizable residue of catalytic importance ($pK_a = 6.9$) that was proposed to be Y155 of the catalytic triad. Amino acid substitutions of the putative catalytic triad residues produced inactive enzymes (S142C, Y155F, Y155E, and K159A) or enzyme with a greatly decreased activity (S142A). Inhibitors were investigated as probes of the molecular features of R-HPC that contribute to substrate binding. 2-[(*S*)-2-Hydroxypropylthio]-ethanesulfonate (S-HPC) and 2-(2-methyl-2-hydroxypropylthio)ethanesulfonate were found to be competitive inhibitors of R-HPC with K_{ic} values close to the K_m for R-HPC. The arginine-specific modifiers 2,3-butanedione and phenylglyoxal were found to be inactivators, and inactivation could be protected against by the addition of R-HPC. 2,3-Butanedione was found to reduce enzyme activity with R-HPC as a substrate much more dramatically than with substrates that lacked a sulfonate moiety [e.g., 2-propanol, (*R*)-2-pentanol, and (*R*)-2-heptanol]. Amino acid analyses of enzyme modified by 2,3-butanedione in the presence and absence of S-HPC suggested protection of a single arginine residue. On the basis of these results, we propose that one or more active site arginines play a key role in substrate binding via an ionic interaction with the sulfonate moiety of R-HPC.

The current trend in the pharmaceutical industry is the synthesis of single enantiomer drugs. This trend was spurred by the realization that single enantiomer drugs can have very different therapeutic properties from their racemates. With the increased demand for chiral pharmaceuticals, there has been a simultaneous increase in the demand for chiral fine chemicals and novel stereoselective catalysts. One approach available to synthetic organic chemists is biocatalysis (*1*), a method that appears to be gaining broader acceptance due to its efficiency and, in some instances, greater economic efficacy.

Chiral alcohols are molecules with a wide range of synthetic applications. The biocatalytic production of chiral alcohols is typified by the asymmetric reduction of the corresponding ketones using purified alcohol dehydrogenase enzymes (*2*). The commercial value of enzymes as stereoselective biocatalysts has been a significant driving force to understand their molecular mechanisms of catalysis and stereoselectivity.

Xanthobacter strain Py2 is a Gram-negative aerobic soil bacterium that utilizes a well-described three-step CO_2- and coenzyme M-dependent pathway for the metabolism of propylene and epoxypropane (Scheme 1) (*3*). Integral to the versatility of this four-enzyme pathway are two stereospecific 2-(2-hydroxypropylthio)ethanesulfonate (HPC)[1] dehydrogenases that individually allow for metabolism of only a single

---

[1] Abbreviations: HPC, 2-(2-hydroxypropylthio)ethanesulfonate; R-HPC, 2-[(*R*)-2-hydroxypropylthio]ethanesulfonate; S-HPC, 2-[(*S*)-2-hydroxypropylthio]ethanesulfonate; coenzyme M, 2-mercaptoethanesulfonate; R-HPCDH, R-HPC dehydrogenase purified from *Xanthobacter* strain Py2; S-HPCDH, S-HPC dehydrogenase purified from *Xanthobacter* strain Py2; rR-HPCDH, recombinant R-HPC dehydrogenase purified from *Escherichia coli*; 2-KPC, 2-(2-ketopropylthio)ethanesulfonate; 2-KPCC, NADPH:2-(2-ketopropylthio)ethanesulfonate oxidoreductase/carboxylase; M-HPC, 2-(2-methyl-2-hydroxypropylthio)-ethanesulfonate; 2-HEC, 2-(2-hydroxyethylthio)ethanesulfonate; Tris, tris(hydroxymethyl)aminomethane; ^{1}H NMR, proton nuclear magnetic resonance spectroscopy; HPLC, high-pressure liquid chromatography; SDS−PAGE, sodium dodecyl sulfate−polyacrylamide gel electrophoresis; SDR, short-chain dehydrogenase/reductase; COB, compulsory-ordered binding.

Scheme 1
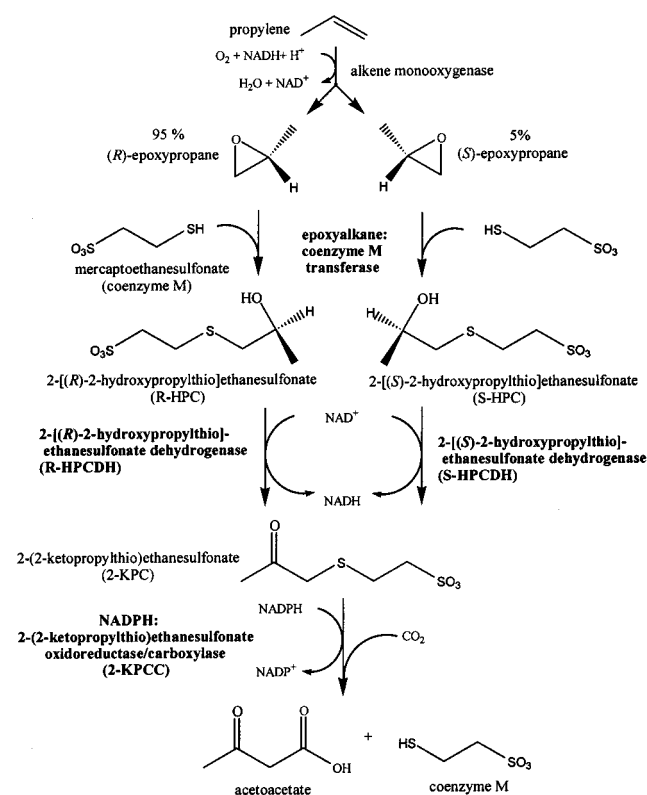
epoxypropane enantiomer (*4*). Collectively, however, these enzymes enable *Xanthobacter* strain Py2 to utilize enantiomeric epoxypropane mixtures, including those produced in vivo by an alkene monooxygenase during growth on gaseous propylene (Scheme 1).

The 2-[(*R*)-2-hydroxypropylthio]ethanesulfonate and 2-[(*S*)-2-hydroxypropylthio]ethanesulfonate dehydrogenases (R-HPCDH and S-HPCDH, respectively) are homologous enzymes that share a relatively high degree of sequence identity (41%) and sequence similarity and belong to the short-chain dehydrogenase/reductase (SDR) superfamily (*4*). Enzymes of this superfamily act on a diverse range of substrates and encompass a wide spectrum of enzymes found in humans, mammals, insects, and bacteria. The defining characteristics of SDR enzymes include a length of approximately 250 amino acids, lack of metal ions, an N-terminal NAD(P)$^+$ binding domain with a conserved GXGXXXG sequence, three highly conserved catalytic residues (serine, tyrosine, and lysine) which constitute a catalytic triad, and a C-terminal domain generally thought to be associated with substrate recognition (*5*, *6*). As part of the current generalized SDR mechanism, the lysine of the catalytic triad is thought to both lower the pK_a of the tyrosine for general base proton abstraction from substrate and bind coenzyme, while the serine is thought to stabilize the anionic character of the substrate transition state via hydrogen bonding.

Although there are currently over 1600 SDR enzymes annotated in databases (*7*), with more than 60 of these characterized biochemically to some degree (*6*), and at least 15 structurally (*8*−*16*), only a few have been discovered that have a homologous partner catalyzing the same reaction but with an opposite stereospecificity. To our knowledge, these enzymes are limited to a set of plant tropinone reductases

(*17*) and two sets of bacterial HPC dehydrogenases (one from *Xanthobacter* strain Py2 and one from *Rhodococcus rhodochrous* B-276) (*3*, *4*). The potential utility of the HPC dehydrogenases as stereoselective biocatalysts, combined with their uniqueness within the SDR superfamily, has warranted further study of their mechanisms of catalysis and enantioselectivity.

In this paper we have cloned the genes (*xecD* and *xecE*) encoding the R- and S-HPCDHs from *Xanthobacter* strain Py2 and expressed them in *Escherichia coli.* While current efforts to render the recombinant S-HPCDH soluble and active have been unsuccessful, the availability of relatively large quantities of recombinant R-HPCDH (rR-HPCDH) has nevertheless made feasible a series of investigations that ultimately intend to address questions regarding the molecular mechanism of stereoselectivity used by this enzyme. To date, very little is known about the R-HPCDH (*3*), other than what has been inferred from sequence similarities to other SDR enzymes and what has been speculated in relation to the plant tropinone reductases (*18*). Therefore, the central aim of this work was to develop the biochemical and kinetic foundation for rR-HPCDH that is a prerequisite to the complete understanding of its mechanism of enantioselectivity. With this in mind, many of the experiments performed herein have indirectly focused on developing a better understanding of substrate binding and specificity of the rR-HPCDH, properties that intuitively are thought to lie at the heart of stereoselectivity. Therefore, we have investigated the kinetic mechanism of the rR-HPCDH using product inhibition, the pH dependence of kinetic parameters for R-HPC, rapid equilibrium inhibitors as probes of substrate specificity, and the possibility of one or more arginine residues involved in substrate binding through the use of chemical modification reagents. Additionally, site-directed mutagenesis has been utilized to confirm previous assumptions based on sequence alignments and to determine if the mechanistic uniformity of other SDR enzymes is observed for rR-HPCDH. The results of these studies are believed to be the first of their kind for an SDR enzyme with a homologue catalyzing the same reaction but with an opposite stereospecificity.

EXPERIMENTAL PROCEDURES

Materials. All organic compounds were purchased from Sigma-Aldrich Chemicals. All other chemicals used were of analytical grade. Compounds not commercially available were synthesized as described below.

Syntheses and Analyses. 2-(2-Ketopropylthio)ethanesulfonate (2-KPC) and HPC enantiomers were synthesized as described previously (*19*). 2-(2-Methyl-2-hydroxypropylthio)ethanesulfonate (M-HPC) and 2-(2-hydroxyethylthio)ethanesulfonate (2-HEC) were prepared in a manner similar to that for the HPC enantiomers with the substitution of either isobutylene oxide or ethylene oxide for propylene oxide in each synthesis, respectively. Using methods described previously (*19*), the purities of all compounds were estimated to be ≥97% using reverse-phase HPLC, and the chemical structures were confirmed using ^{1}H NMR. The spectra of HPC enantiomers and 2-KPC demonstrated resonances with splitting, chemical shifts, and integrations identical to those reported previously (*3*, *19*). The spectrum of M-HPC

demonstrated four signals: a singlet at 1.26 ppm that integrated to six protons, a singlet at 2.74 ppm that integrated to two protons, and multiplets centered at 2.89 and 3.13 ppm that each integrated to two protons. The spectrum of 2-HEC was composed of four multiplets that each integrated to two protons and were centered on the following shift values: 2.74, 2.87, 3.13, and 3.72 ppm.

Cloning of the R-HPCDH and S-HPCDH Genes (xecD and xecE). Total genomic DNA was isolated from propylene-grown cells of *Xanthobacter* strain Py2 as described previously (*20*). For the cloning of *xecD*, PCR reactions were set up that contained 100 ng of *Xanthobacter* strain Py2 genomic DNA, 1.0 μM primers (forward, CATATGAGCCGCGTCGC-CATTGTCAC; reverse, GGATCCTCAGATGGCGGTG-TAAGCGCCA), 12% glycerol, and a PCR bead (Amersham Pharmacia Biotech) that supplied *Taq* polymerase, dNTP's, and buffer. Touch-down PCR was carried out using the following cycling parameters: stage 1, (94 °C × 5 min) × 1; stage 2, (94 °C × 15 s, 70 °C × 30 s [$\Delta - 2$ °C·cycle^{-1}], 72 °C × 30 s) × 25; stage 3, (94 °C × 15 s, 50 °C × 30 s, 72 °C × 30 s) × 20; stage 4, (72 °C × 7 min) × 1. For the cloning of *xecE*, PCR reactions were set up that contained 100 ng of *Xanthobacter* strain Py2 genomic DNA, 0.1 μM primers (forward, CATATGCTGGACGCAGAGGTCATCG; reverse, GGATCCTCAGATTGCGGTCATCCCGCCATC), 15% glycerol, and a PCR bead. Touch-down PCR was carried out as for *xecD*. The cloning procedures for both *xecD* and *xecE* were identical, and for simplicity, this procedure is described below in terms of *xecD* only.

The PCR products were resolved on a 1% agarose gel, and *xecD* DNA (0.75 kb) was extracted using the QIAEX II gel extraction kit (Qiagen Inc.). Purified *xecD* DNA was ligated into the pGEM-T cloning vector (Promega) to generate plasmid pXDT. pXDT and the pET28-b expression vector (Novagen) were simultaneously subjected to a double digest with *Nde*I and *Bam*HI, and pET28-b was then dephosphorylated using calf intestinal alkaline phosphatase. Digested plasmids were resolved on a 1% agarose gel, and *xecD* and pET28-b DNA were extracted using the QIAEX II gel extraction kit. Purified *xecD* and pET28-b DNA were ligated with T4 DNA ligase overnight at 4 °C to generate plasmid pXD28 that was subsequently transformed into *E. coli* JM109 for plasmid maintenance and into *E. coli* BL21-(DE3) CodonPlus (Stratagene) cells for expression. pXD28 was isolated from *E. coli* JM109 for insert confirmation by DNA sequencing.

Site-Directed Mutagenesis (SDM). All oligonucleotides utilized for SDM were purchased from MWG Biotech. SDM of pXD28 was carried out utilizing the Quickchange site-directed mutagenesis kit (Stratagene) according to the manufacturer's protocols. All mutations were confirmed by DNA sequencing. The sequences of the mutagenic primer pairs utilized for each codon substitution in *xecD* are as follows: S142A, ATCGTCAACATCGCCGCGGTCGC-GAGCCTCGTC and GACGAGGCTCGCGACCGCGGC-GATGTTGACGAT; S142C, ATCGTCAACATCGCCT-GCGTCGCGAGCCTCGTC and GACGAGGCTCGCG-ACGCAGGCGATGTTGACGAT; Y155F, CCGGGGCG-CTCCGCCTTCACCACCTCCAAGGGG and CCCCTT-GGAGGTGGTGAAGGCGGAGCGCCCCGG; Y155E, CC-GGGGCGCTCCGCCGAAACCACCTCCAAGGGG and

CCCCTTGGAGGTGGTTTCGGCGGAGCGCCCCGG; K-159A, GCCTACACCACCTCCGCGGGGGCGGTGCTG-CAG and CTGCAGCACCGCCCCCGCGGAGGTGGTG-TAGGC.

DNA Sequencing. All DNA sequencing was performed on PE/ABI 377 and 373A stretch sequencers with Taq FS terminator chemistry at the Utah State University Biotechnology Center DNA sequencing laboratory. The following sequencing primer was used to confirm all mutations to pXD28: ACGCCCGTCGAGCAGTTCGACAAG.

Growth Media. E. coli JM109 was grown in standard Luria–Bertani (LB) broth containing either ampicillin (100 μg·mL^{-1}) or kanamycin (50 μg·mL^{-1}). *E. coli* BL21(DE3) CodonPlus was grown in LB-rich media that contained the following components per liter: 20 g of tryptone, 15 g of yeast extract, 2 g of K$_2$HPO$_4$, 1 g of KH$_2$PO$_4$, 8 g of NaCl, and 10 g of glucose (1% v/v). LB-rich media was supplemented with kanamycin (50 μg·mL^{-1}) and chloramphenicol (50 μg·mL^{-1}).

Growth of Bacteria. All bacteria were grown at 37 °C unless otherwise stated. *E. coli* BL21(DE3) CodonPlus cells were transformed with the pXD28 or corresponding mutant plasmid according to the manufacturer's recommendations and then plated and grown overnight. A single colony from this plate was used to grow a 25 mL liquid culture to an A_{600} of 0.6 for preparation of 15% glycerol (v/v) stocks that were stored at −80 °C until use. For use, cells from a frozen stock were plated and grown overnight. Colonies were removed from the overnight plate, inoculated into 250 mL of LB-rich media, and grown to an A_{600} between 0.6 and 1.0. This culture was used as the inoculum for a 15 L capacity microferm fermentor (New Brunswick Scientific) containing 11 L of LB-rich media supplemented with antifoam A (0.005% v/v). Cells were allowed to grow at 30 °C with stirring at 400 rpm with forced aeration to an A_{600} between 0.6 and 1.0. At this time, 2-mercaptoethanol was added to an overall concentration of 1 mM, and the fermentor was rapidly cooled to 15 °C. At 15 °C, IPTG was added to an overall concentration of 0.25 mM, and cells were allowed to grow at this temperature for 4−5 h. Cells were concentrated using a tangential flow filtration system (Millipore Corp.) and pelleted by centrifugation. Cell paste was drop frozen in liquid nitrogen and stored at −80 °C.

Preparation of Cell-Free Extracts. One hundred grams of frozen cell paste was thawed at room temperature in 2 volumes of lysis buffer (20 mM Tris, 25% glycerol, 500 mM NaCl, 25 mM imidazole, 0.03 mg·mL^{-1} DNase I, at pH 8.0). This mixture was homogenized and subjected to two passes through a French pressure cell at 15000 psi. Cell extract was centrifuged (4000*g*) for 60 min, and the supernatant (clarified cell extract) was retained for purification.

Purification of R-HPCDH, rR-HPCDH, and rR-HPCDH Mutants. R-HPCDH was purified from propylene-grown *Xanthobacter* strain Py2 as described previously (*21*). For the purification of rR-HPCDH and rR-HPCDH mutants, clarified cell extract (produced from 100 g of cell paste) was applied to a 2.5 × 3.2 cm column of Ni-NTA Superflow (QIAGEN) at 4.0 mL·min^{-1} (48.9 cm·h^{-1}). The column was rinsed with 1 column volume of lysis buffer, followed by 10 column volumes of rinse buffer (20 mM Tris, 25%

glycerol, 500 mM NaCl, 50 mM imidazole pH 8.0). rR-HPCDH was eluted using three column volumes of elution buffer (20 mM Tris, 25% glycerol, 500 mM NaCl, 500 mM imidazole) and dialyzed (6−8000 MW cutoff) against 5 L of 50 mM Tris, 100 mM NaCl, and 10% glycerol, pH 8.2, overnight; for the S142C variant of R-HPC, 2 mM dithiothreitol was included in the dialysis buffer. Dialyzed protein was concentrated over a 30000 MW cutoff membrane to ≥3.5 mg·mL^{-1} and drop frozen in liquid nitrogen for storage at −80 °C. All steps were performed at 4 °C. Protein concentrations were determined using a modified biuret assay with bovine serum albumin as the standard (*22*).

SDS−PAGE and Native PAGE Analysis. SDS−PAGE (12% T) and native PAGE (10% T) were performed following the Laemmli procedure (*23*). Proteins were visualized by staining with Coomassie blue. The apparent molecular masses of polypeptides on SDS−PAGE gels were determined by comparison to R_f values of standard proteins. The relative migration of mutant rR-HPCDHs on native PAGE gels was compared directly to flanking standards of wild-type rR-HPCDH.

Determination of rR-HPCDH and rR-HPCDH Mutant Native Molecular Masses. The native molecular masses of rR-HPCDH and rR-HPCDH mutants were estimated by gel filtration chromatography using a Pharmacia Superose 12 HR 10/30 column equilibrated in 50 mM NaHPO$_4$, pH 7.5, containing 200 mM NaCl. The column was calibrated with alcohol dehydrogenase (150 kDa), bovine serum albumin (66 kDa), ovalbumin (45 kDa), carbonic anhydrase (31 kDa), and cytochrome *c* (12.3 kDa). All separations were performed at a flow rate of 0.2 mL·min^{-1}. A calibration curve was constructed by plotting the log of the native molecular mass for standards on the *y*-axis against the V_e/V_o value on the *x*-axis, where V_e and V_o are the protein elution and column void volumes, respectively. This plot was fit using linear regression, and the equation of this line was used to determine the log native molecular masses for rR-HPCDH and rR-HPCDH mutants using their experimentally determined V_e/V_o values.

Circular Dichroism (CD). CD spectra (190−300 nm) were recorded at 25 °C on an AVIV model 62DS CD spectrometer. Samples were prepared in buffer containing 10 mM KH$_2$PO$_4$ and 100 mM KF at pH 7.0, with overall enzyme concentrations of approximately 0.3 mg·mL^{-1} (10 μM). Analyses were performed on the average of five scans, and the residue ellipticity (θ) was calculated using 270 amino acid residues. In all cases, a 0.1 cm path length and 1 nm spectral bandwidth were used.

Enzyme Assays and Data Analysis. All enzyme assays were performed at 30 °C in a Shimadzu model UV160U spectrophotometer containing a water-jacketed cell holder for thermal control. Assays were initiated by the addition of enzyme, and the ΔA_{340nm}·min^{-1} for NADH was correlated with either micromoles of R-HPC oxidized or micromoles of 2-KPC reduced using the extinction coefficient for NADH (ϵ_{340} = 6.22 mM^{-1}·cm^{-1}). Kinetic constants (K_m and V_{max}) were calculated by fitting initial rate data to the appropriate equation using the software SIGMAPLOT.

Standardization of Stock Solutions. Stock solutions of 2-[(*R*)-2-hydroxypropylthio]ethanesulfonate (R-HPC) and 2-[(*S*)-2-hydroxypropylthio]ethanesulfonate (S-HPC) were standardized by use of the rR-HPCDH and S-HPCDH

[purified as described previously(*21*)], respectively. In either case, assays contained enzyme (100 μg), 10 mM NAD$^+$, and variable concentrations of HPC enantiomer in GPT buffer mix (50 mM glycine, 50 mM NaHPO$_4$, 50 mM Tris base) at pH 11.0 (a pH that renders both enzymes irreversible). Standardization assays were performed in triplicate and were started by the addition of an aliquot of the corresponding enantiomer of HPC from a stock solution. Reactions were allowed to proceed for 2 min. The average absorbance at 340 nm for NADH was correlated with micromoles of either R- or S-HPC present in stock solution aliquots. Stock solutions of NADH and NAD$^+$ were standardized using the extinction coefficients for NADH at 340 nm (ϵ = 6.22 mM·cm^{-1}) and NAD$^+$ at 260 nm (ϵ = 18.0 mM·cm^{-1}).

Initial Velocity Studies in the Absence of Products or Inhibitors. All assays were performed in GPT buffer mix at pH 7.5. In preparing this buffer mixture, it was found that assays performed in either glycine, phosphate, or Tris alone, at pH values close to the respective pK_a values, gave rates that were indistinguishable from assays conducted in GPT buffer at the same pH value. Kinetic parameters for the oxidation of R-HPC were determined by varying the concentration of R-HPC at several fixed concentrations of NAD$^+$ and the converse experiment where NAD$^+$ was the variable substrate at several fixed concentrations of R-HPC. Initial rate data were fit to the equation:

$$v^f = (V^f_{max}[\text{NAD}^+][\text{R-HPC}])/$$
$$((K_{dNAD^+}K_{mR-HPC}) + (K_{mNAD^+}[\text{R-HPC}]) +$$
$$(K_{mR-HPC}[\text{NAD}^+]) + ([\text{NAD}^+][\text{R-HPC}])) \quad (1)$$

where V^f_{max} is the maximal rate for the forward reaction when both substrates are saturating and K_{dNAD} is the dissociation constant for the outermost substrate, NAD$^+$.

Estimation of the Equilibrium Constant at pH 7.5. All assays were performed in GPT buffer mix at pH 7.5. Kinetic parameters for the reverse reaction (NADH-dependent 2-KPC reduction) were determined by varying NADH (27, 54, 82, 127, 163 μM) at a single saturating concentration of 2-KPC (500 μM) and varying 2-KPC (25, 50, 100, 200, 350, 500 μM) at a single saturating concentration of NADH (163 μM). The kinetic parameters for the forward and reverse reactions were used to estimate the equilibrium constant at pH 7.5 according to the Haldane relationship for a bisubstrate enzyme reaction:

$$K_{eq} = (V^f_{max}K_{mNADH}K_{m2-KPC})/(V^r_{max}K_{mNAD^+}K_{mR-HPC}) \quad (2)$$

where V^f_{max} and V^r_{max} are the maximal rates for the forward and reverse reactions, respectively, when both substrates are saturating.

pH Dependence of Kinetic Parameters. Kinetic parameters for R-HPC were determined in GPT buffer mix (pH 6.0, 6.5, 7.0, 7.5, 8.0, 8.5, 9.0, 9.5, and 10.0) or APT buffer mix (50 mM CH$_3$COONa, 50 mM NaH$_2$PO$_4$, and 50 mM Tris base) (pH 5.0, and 5.5) adjusted to the desired pH at 30 °C. In all experiments, R-HPC was the variable substrate and NAD$^+$ remained at a fixed concentration of 10 mM (saturating over the entire pH range of the study). Comparison of the maximal specific activities at pH 6.0 in GPT and APT

buffer mixes indicated that APT mix supported higher activities. Therefore, for normalization purposes, the ratio of the maximal specific activity at pH 6.0 in GPT mix to that in APT mix was multiplied by all specific activities determined at pH 5.0 and 5.5 in APT mix. The effect of pH on the ionization of free enzyme was visualized by constructing a plot of k_{cat}/K_m vs pH. This plot was fit to eq 3 that assumes a drop in k_{cat}/K_m at low pH (*24*):

$$\log k_{cat}/K_m = \log(C/(1 + [H^+]/K_a)) \qquad (3)$$

where *C* is the maximal log k_{cat}/K_m value and K_a is the acid dissociation constant of the catalytically important ionizing residue. log k_{cat} and log K_m vs pH plots were constructed in a point-to-point manner.

Initial Velocity Studies in the Presence of Rapid Equilibrium Inhibitors. All assays were performed in GPT buffer mix at pH 7.5 with saturating NAD$^+$ (5 mM) and variable concentrations of R-HPC (75, 165, 350, 645, and 1010 μM). Each assay was performed with five fixed concentrations of inhibitor: S-HPC (0, 200, 500, 1000, 2000 μM); M-HPC (0, 200, 500, 1000, 2000 μM); mercaptoethanesulfonate (0, 2, 5, 10, 20 mM); ethanesulfonate (0, 10, 20, 50, 100 mM); methanesulfonate (0, 19.8, 49.5, 99, 198 mM). Initial rate data for each inhibitor were fitted to the following equations describing enzyme activity in the presence of competitive (eq 4), uncompetitive (eq 5), and mixed inhibitors (eq 6):

$$v = V_{max}[S]/(\alpha K_m + [S]) \qquad (4)$$

$$v = V_{max}[S]/(K_m + \alpha'[S]) \qquad (5)$$

$$v = V_{max}[S]/(\alpha K_m + \alpha'[S]) \qquad (6)$$

where S is the substrate, I is the inhibitor, $\alpha = 1 + ([I]/K_{ic})$, and $\alpha' = 1 + ([I]/K_{iu})$. The type of inhibition exhibited for each compound was determined by graphing initial rate data in the form of double reciprocal plots ($1/v$ vs $1/[S]$ at various [I]) and Dixon plots ($1/v$ vs [I]) and by comparing actual values to the theoretical values generated using SIGMA-PLOT for each possible type of inhibition. The types of inhibition exhibited for the products of R-HPC oxidation (NADH and 2-KPC) were determined in a similar manner.

Time- and Concentration-Dependent Inactivation of rR-HPCDH with 2,3-Butanedione. Three hundred microliters of rR-HPCDH (3.8 mg·mL^{-1}) was desalted into 3 mL using a PD-10 column (Amersham Pharmacia Biotech; Sephadex G-25 M) equilibrated in 50 mM sodium borate, pH 9.0. Aliquots (0.2 mL) of desalted rR-HPCDH were incubated (under normal laboratory fluorescent lighting conditions) in crimp-sealed serum vials (3 mL) at 25 °C that contained different concentrations of 2,3-butanedione (0, 2.5, 5.0, 10, 15, 20, 30, and 40 mM). All modification reactions were started by the addition of 2,3-butanedione. Aliquots (10 μL) were removed from modification reactions at fixed times (1, 10, 20, 30, 40, 50, 60 min) to determine R-HPC oxidation activity in assays that contained 5 mM NAD$^+$ and 5 mM R-HPC. All activity assays used GPT buffer mix, pH 7.5, and had an overall volume of 1 mL. Percent activities were calculated by dividing the activity following modification (at time *t*) by the activity (at time *t*) of unmodified enzyme. Pseudo-first-order rate constants of inactivation (at each 2,3-

butanedione concentration) were determined by plotting percent activity versus time on a semilog plot with data fit to the equation:

$$A = A_0 e^{-kt} \qquad (7)$$

where *A* is the percent activity at time *t*, A_0 is the activity at time zero, and *k* is the pseudo-first-order rate constant of inactivation. A plot of log *k* versus the log of the 2,3-butanedione concentration was constructed and fit to a straight line using linear regression analysis to confirm the order of the reaction with respect to 2,3-butanedione (*25*). Pseudo-first-order rate constants of inactivation (*k*) with units of inverse seconds were plotted against the concentration of 2,3-butanedione (molar) and fit to a straight line using linear regression. The slope of this plot yielded the true second-order rate constant of inactivation with units of M^{-1} s^{-1}.

Substrate Protection Experiments with 2,3-Butanedione and Phenylglyoxal. Two hundred and twenty-five microliters of rR-HPCDH (5 mg·mL^{-1}) was desalted into 3 mL using a PD-10 column equilibrated in 50 mM sodium borate, pH 9.0. Aliquots (0.2 mL) of desalted rR-HPCDH were then incubated at 25 °C in crimp-sealed 3 mL serum vials under varied combinations of arginine modifier (2,3-butanedione or phenylglyoxal) and protectant. End point enzyme activity assays were performed after 30 min by removing 10 μL aliquots from reaction vials. Activity assays were carried out in duplicate under saturating concentrations of NAD$^+$ (5 mM) and R-HPC (5 mM) in GPT buffer mix at pH 7.5. Data were used to calculate percent protection using the equation (*26*):

% protection =
$$[(\% \text{ act}_{presence} - \% \text{ act}_{absence})/(100 - \% \text{ act}_{absence})] \times 100 \qquad (8)$$

where % act$_{presence}$ and % act$_{absence}$ are the percentages of the original activity in the presence and absence of a protector, respectively.

Preparation of Samples for Amino Acid Analysis. Four hundred and fifty microliters of rR-HPCDH (5 mg·mL^{-1}) was desalted into 3 mL using a PD-10 column equilibrated in 50 mM sodium borate, pH 9.0. Samples (0.9 mL) of desalted rR-HPCDH were incubated at 30 °C in crimp-sealed serum vials (3 mL) under three different conditions: no additions, 40 mM 2,3-butanedione, and 40 mM 2,3-butanedione with 150 mM S-HPC, each in 50 mM sodium borate, pH 9.0, with total volumes of 1.25 mL. After 30 min, 0.5 mL of 1 M NaBH$_4$ was added to each vial (to reduce and trap arginine-modified complexes) followed by incubation at room temperature for 10 min. A quantity of each sample (2.5 mL) was then desalted into 3 mL using PD-10 columns (equilibrated in deionized water). Desalted samples were drop frozen in liquid nitrogen and shipped on dry ice to the amino acid analysis staff of the University of Nebraska Medical College Protein Structure Core Facility located in Omaha, NE.

Activity of 2,3-Butanedione-Treated rR-HPCDH with Alternative Substrates. Samples (1.5 mL) of rR-HPCDH (6.36 mg·mL^{-1}) were desalted into 3 mL using a PD-10 column equilibrated in 50 mM sodium borate, pH 9.0. This was repeated, and the desalted rR-HPCDH fractions were pooled. Aliquots (2.5 mL) of this pool were incubated at 25

°C in crimp-sealed serum vials (9 mL) with and without 40 mM 2,3-butanedione in total volumes of 3 mL. After 45 min, a 2.5 mL aliquot was removed from each reaction vial and desalted into 3 mL using a parallel PD-10 column equilibrated in "stabilization buffer" containing 50 mM sodium borate, 100 mM KCl, 5% v/v polyethylenimine, and 5 mg·mL^{-1} bovine serum albumin at pH 9.0. Relative protein concentrations were compared using a modified biuret method for normalization purposes (*22*). Activity assays with subsaturating quantities (defined as 1 K_m) of R-HPC, 2-propanol, (*R*)-pentanol, and (*R*)-heptanol were performed using 8.1 μg of rR-HPCDH and 10 mM NAD$^+$ in GPT buffer mix at pH 7.5.

RESULTS

Production of rR-HPCDH. rR-HPCDH was produced only in BL21(DE3) CodonPlus cells (Stratagene), a strain that harbors a plasmid encoding tRNAs for rare codons used by *E. coli*. Examination of the codon usage in the *xecD* gene supported this observation with the finding that three rare codons were present, one for arginine (AGG) and two for proline (CCC). This hinted that codon biasing may have contributed to the lack of expression observed in more conventional BL21(DE3) expression strains. The expression and purification protocol described in this work typically yielded ≥1.0 mg of soluble active rR-HPCDH/g of *E. coli* compared to average R-HPCDH yields of ≤0.2 mg of protein/g of propylene-grown *Xanthobacter* strain Py2 reported previously (*21*).

Production of rS-HPCDH. rS-HPCDH was expressed at levels equivalent to that of the rR-HPCDH in *E. coli* BL21-(DE3) CodonPlus cells under identical conditions. However, under these conditions, all of the rS-HPCDH produced was insoluble and consequently inactive. Attempts to remedy rS-HPCDH insolubility by decreasing the induction temperature to as low as 5 °C, varying the time of induction (A_{600}), varying the IPTG concentration, varying the media composition (expression in LB media supplemented with 1 M sorbitol and betaine), and combinations of each were unsuccessful (*27*).

Comparisons of R-HPCDH, rR-HPCDH, and rR-HPCDH Mutants. Native molecular mass, estimated by gel filtration chromatography, indicated that the rR-HPCDH migrated as a dimer with an apparent value of 63.9 kDa. This closely matched the published value (64.8 kDa) for the R-HPCDH (*21*) and, because so, indicated that inclusion of the N-terminal six-histidine tag did not affect dimerization of the recombinant protein. Moreover, side-by-side enzyme activity assays with rR-HPCDH and R-HPCDH, under conditions of saturating substrates, indicated that inclusion of the histidine tag did not compromise maximal recombinant enzyme activity. These data supported the use of the recombinant enzyme in this work over the R-HPCDH that requires a more laborious purification strategy and gives a comparatively lower yield.

SDS−PAGE analysis of rR-HPCDH and rR-HPCDH mutants estimated the average purities of the enzymes used in this work to be ≥95%. As expected with the inclusion of 20 additional amino acids on their N-termini (vector-encoded histidine tag, thrombin cutting site, etc.), the recombinant proteins migrated on SDS−PAGE gels as single bands with
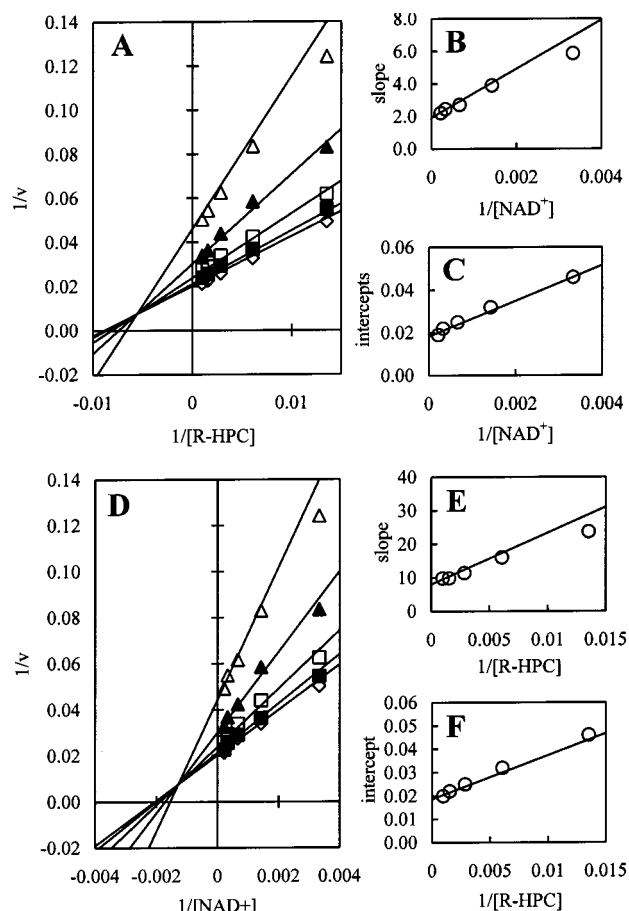

FIGURE 1: (A, D) Double reciprocal plots of rR-HPCDH catalyzed oxidation of 2-[(*R*)-2-hydroxypropylthio]ethanesulfonate (R-HPC) at 30 °C and pH 7.5. (A) $1/v$ as a function of the inverse R-HPC concentration determined at several fixed concentrations of NAD$^+$: (△) 300, (▲) 700, (□) 1500, (■) 3000, and (◇) 4500 μM. (D) $1/v$ as a function of inverse NAD$^+$ concentration determined at several fixed concentrations of R-HPC: (△) 74, (▲) 164, (□) 350, (■) 643, and (◇) 1010 μM. (B, C, E, F) Secondary plots of (A) and (D) further illustrating data quality and fit to eq 1. (B) Slopes from plot A as a function of the inverse NAD$^+$ concentration. (C) Intercepts from plot A as a function of the inverse NAD$^+$ concentration. (E) Slopes from plot D as a function of the inverse R-HPC concentration. (F) Intercepts from plot D as a function of the inverse R-HPC concentration. Data points represent the average of triplicate experiments. In all cases lines represent linear regression of SIGMAPLOT generated theoretical data.

slightly higher molecular masses than R-HPCDH. Interestingly, it was previously shown that highly purified R-HPCDH migrates as two bands on SDS−PAGE gels (*21*), presumably due to protein degradation, although protease inhibitors could not prevent this result (*21*). This finding may indicate that the recombinant dehydrogenase has a special resistance to similar degradation or simply that the preparation and purification of the recombinant enzyme do not result in exposure to these destructive conditions.

Native PAGE, gel filtration chromatography, and CD spectrapolarimetric analyses were performed on all rR-HPCDH mutants (S142A, S142C, Y155F, Y155E, and K159A) in parallel with wild-type rR-HPCDH. Native PAGE results indicated that all of the rR-HPCDH mutants migrated in a manner similar to that of the wild-type rR-HPCDH. Gel filtration chromatography was performed on all rR-HPCDH mutants and indicated that all migrated as dimers with molecular mass values identical to that of the wild-type
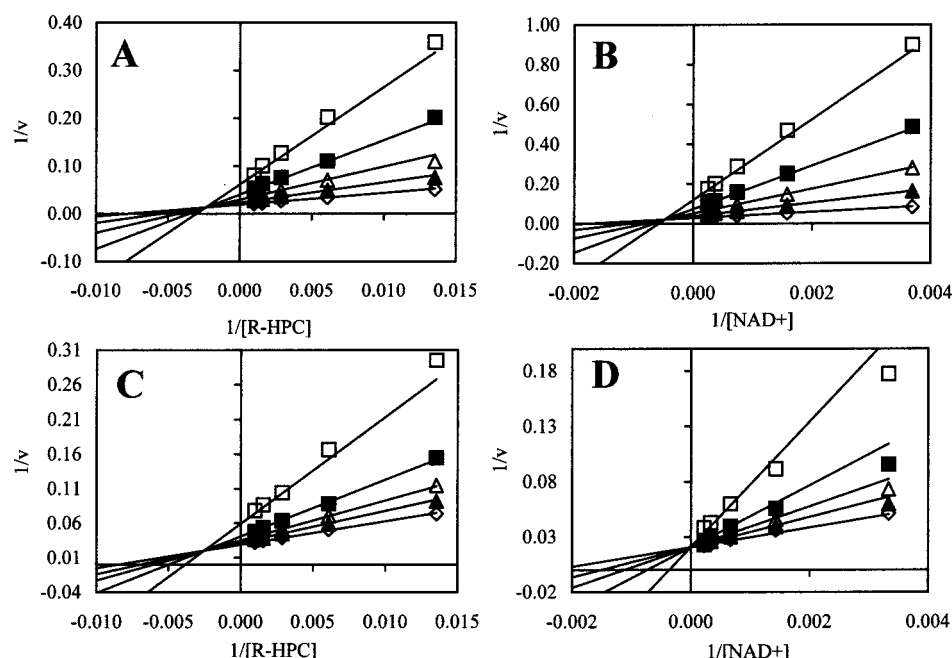
FIGURE 2: Double reciprocal plots illustrating product inhibition of rR-HPCDH during 2-[(R)-2-hydroxypropylthio]ethanesulfonate (R-HPC) oxidation. Abbreviation: 2-KPC, 2-(2-ketopropylthio)ethanesulfonate. (A) 2-KPC as a mixed inhibitor with respect to R-HPC. (B) 2-KPC as a mixed inhibitor with respect to NAD$^+$. (C) NADH as a mixed inhibitor with respect to R-HPC. (D) NADH as a competitive inhibitor with respect to NAD$^+$. The concentrations of 2-KPC in plots A and B are as follows: (◇) no 2-KPC added and (▲) 100, (△) 250, (■) 500, and (□) 1000 μM 2-KPC. The concentrations of NADH in plots C and D are as follows: (◇) no NADH added and (▲) 22, (△) 44, (■) 89, and (□) 224 μM NADH. Data points represent the average of triplicate experiments. In all cases lines represent linear regression of SIGMAPLOT generated theoretical data for the respective type of inhibition, where plots A, B, and C were fit to eq 6 and plot D was fit to eq 4.

recombinant enzyme. CD analyses revealed that the rR-HPCDH mutants produced spectra identical to that of the wild-type enzyme. Collectively, these data suggested that the perturbation, or elimination of, activity exhibited for the rR-HPCDH mutants (Table 3) was the result of changes in the chemical properties of their amino acid side chains and not drastic alterations in structure.

Initial Velocity Studies in the Absence of Products or Inhibitors. Double reciprocal plots of initial rate data from bisubstrate kinetic experiments indicated that when the concentration of R-HPC was varied at several fixed concentrations of NAD$^+$ (Figure 1A), and vice versa (Figure 1D), the lines in both cases intersected to the left of the y-axis. This classic kinetic pattern was consistent with a ternary complex enzyme mechanism defined by the requirement that both substrates must meet on the enzyme for the reaction to occur (*25*, *28*). The slopes and intercepts from panels A and D of Figure 1 were used to construct four secondary plots (Figure 1B,C,E,F) to show both data quality and fit to eq 1. Data fitting allowed calculation of the following kinetic parameters for rR-HPCDH-catalyzed R-HPC oxidation at pH 7.5: V_{max}, 54.7 ± 0.9 units·mg^{-1}; k_{cat}, 25.8 s^{-1}; K_m for R-HPC, 105 ± 2 μM; K_m for NAD$^+$, 457 ± 12 μM; K_d for NAD$^+$, 180 ± 4 μM. The kinetic parameters for the reverse reaction (2-KPC reduction) were determined at pH 7.5: V_{max}, 51.9 ± 0.5 units·mg^{-1}; k_{cat}, 24.5 s^{-1}; K_m for 2-KPC, 92 ± 3 μM; K_m for NADH, 36.6 ± 0.3 μM. Using the Haldane relationship for a bisubstrate enzyme (eq 2), the equilibrium constant was determined to be 7.5 × 10^{-2} at 30 °C and pH 7.5.

Initial Velocity Studies with a R-HPC Analogue. To investigate the importance of the terminal methyl group of R-HPC to binding and turnover, 2-HEC, an analogue of R-HPC that lacks a terminal methyl group, was prepared and used as a substrate. Kinetic parameters for rR-HPCDH with variable 2-HEC and a fixed saturating concentration of NAD$^+$ (10 mM) at pH 7.5 were determined as follows: V_{max}, 0.607 ± 0.006 units·mg^{-1}; k_{cat}, 0.29 s^{-1}; K_m, 750 ± 40 μM; k_{cat}/K_m, 3.8 × 10^2 M^{-1}·s^{-1}.

Initial Velocity Studies in the Presence of Products. Product inhibition of rR-HPCDH-catalyzed R-HPC oxidation was utilized in an attempt to elucidate the kinetic mechanism. Panels A−D of Figure 2 are double reciprocal plots that illustrate the fit of initial rate data in the presence of a product inhibitor to a particular type of rapid equilibrium inhibition. For each of these figures, the type of product inhibition, the concentration of the fixed substrate, and the calculated inhibition constants are summarized in Table 1.

2-KPC was found to be a mixed inhibitor with respect to both R-HPC and NAD$^+$, providing values of K_{ic} comparable to the K_m for 2-KPC (92 ± 3 μM) obtained for the reverse reaction under conditions of saturating NADH. The K_{ic} values for 2-KPC, determined by these two experiments, likely describe the formation of nonproductive NAD$^+$·2-KPC complexes under two different conditions.

NADH was a mixed inhibitor with respect to R-HPC, with a K_{ic} value comparable to the determined K_m for NADH (36.6 ± 0.3 μM) in the reverse reaction when 2-KPC was saturating. NADH was found to be a competitive inhibitor vs NAD$^+$, and the K_{ic} value was again comparable to the K_{ic} measured with R-HPC as the variable substrate and the K_m for NADH in the reverse direction. The K_{ic} values for NADH determined by these two experiments likely describe the equilibrium of NADH with free enzyme under two different conditions. In summary, the patterns of product

Table 1: Summary of the Product Inhibition Observed for the rR-HPCDH during 2-[(R)-2-Hydroxypropylthio]ethanesulfonate (R-HPC) Oxidation at pH 7.5

reference	product inhibitor	variable substrate	fixed substrate	[fixed substrate] (mM)	inhibition	inhibition constants K_{ic} (μM)	K_{iu} (μM)
Figure 2A	2-KPC	R-HPC	NAD$^+$	5.0^a	mixed	137 ± 1	448 ± 8
Figure 2B	2-KPC	NAD$^+$	R-HPC	0.2^b	mixed	83 ± 2	309 ± 8
Figure 2C	NADH	R-HPC	NAD$^+$	1.0^b	mixed	63 ± 1	215 ± 3
Figure 2D	NADH	NAD$^+$	R-HPC	1.0^a	competitive	42 ± 1	NA

^{a} Concentration equal to 10 times the K_m. ^{b} Concentration equal to 2 times the K_m. Abbreviation: 2-KPC, 2-(2-ketopropylthio)ethanesulfonate. All inhibition constants are listed as means ± standard deviations.

Table 2: pH Dependence of Kinetic Parameters for the rR-HPCDH-Catalyzed Oxidation of 2-[(R)-2-Hydroxypropylthio]ethanesulfonate (R-HPC)^a

pH	V_{max} (units·mg^{-1})	K_m (μM) R-HPC	k_{cat} (s^{-1})	k_{cat}/K_m (M^{-1}·s^{-1})
5.0	13.1 ± 0.1	1270 ± 20	6.2	4.9 × 10^3
5.5	17.9 ± 0.4	660 ± 30	8.4	1.3 × 10^4
6.0	22.5 ± 0.3	194 ± 3	10.6	5.5 × 10^4
6.5	31.6 ± 0.2	174 ± 3	14.9	8.6 × 10^4
7.0	43 ± 1	118 ± 4	20.2	1.7 × 10^5
7.5	56.8 ± 0.5	102 ± 2	26.8	2.6 × 10^5
8.0	62 ± 1	102 ± 7	29.1	2.8 × 10^5
8.5	66.5 ± 0.4	89 ± 3	31.4	3.5 × 10^5
9.0	75.9 ± 0.3	106 ± 5	35.8	3.4 × 10^5
9.5	82 ± 1	108 ± 3	38.5	3.6 × 10^5
10.0	84 ± 2	115 ± 7	39.4	3.4 × 10^5

^{a} Abbreviations: R-HPC, 2-[(R)-2-hydroxypropylthio]ethanesulfonate. All assays were performed in triplicate at 30 °C with a fixed saturating concentration of NAD$^+$ (10 mM). One unit of enzyme activity was defined as 1 μmol of R-HPC oxidized per minute. k_{cat} and k_{cat}/K_m values were calculated using average V_{max} and K_m values as listed. V_{max} and K_m values are given as means ± standard deviations. All other values are given as means only.

FIGURE 3: Variation of k_{cat} (A), k_{cat}/K_{mR-HPC} (B), and K_{mR-HPC} (C) with pH for rR-HPCDH-catalyzed R-HPC oxidation. Lines in (A) and (C) are point-to-point connections. The line in (B) represents data fit to eq 3. Data fitting of (B) indicated the ionization of a single group on the free enzyme with a pK_a of 6.9. All values used to construct plots were identical to those found in Table 2.

inhibition are consistent with a compulsory-ordered binding (COB) mechanism with NAD$^+$ binding first (*25, 28, 29*).

pH Dependence of Kinetic Parameters. Table 2 summarizes the pH dependence of kinetic parameters for the rR-HPCDH when R-HPC was the variable substrate and NAD$^+$ was saturating. The data were plotted in three forms in order to gain insights into the chemical mechanism: log k_{cat} vs pH, log k_{cat}/K_m vs pH, and log K_m vs pH (Figure 3). The experimental data points of each plot in Figure 3, represented by pH 5.0, 5.5, and 6.0, were fit using linear regression. The fits indicated the following slope and correlation coefficient (R^2) values: Figure 3A, slope of 0.233 with an R^2 value of 0.994; Figure 3B, slope of 1.049 with an R^2 value of 0.988; Figure 3C, slope of −0.816 with an R^2 value of 0.970.

Site-Directed Mutagenesis. A summary of the amino acid substitutions to the catalytic triad, along with their effects on the kinetic parameters of the enzyme, when R-HPC was the variable substrate (and NAD$^+$ was the fixed saturating substrate), is presented in Table 3. As shown, Y155F, Y155E, S142C, and K159A mutants were completely inactive. In contrast, the S142A mutant exhibited a low level of activity, with a k_{cat} value 120-fold lower than the wild-type enzyme and a $K_{m R-HPC}$ value that was 8-fold higher.

Initial Velocity Studies in the Presence of Rapid Equilibrium Inhibitors. A variety of rapid equilibrium inhibitors were investigated as probes for the important molecular features of R-HPC that contribute to recognition and binding affinity. These compounds with their structures, modes of inhibition, and experimentally determined inhibition constants
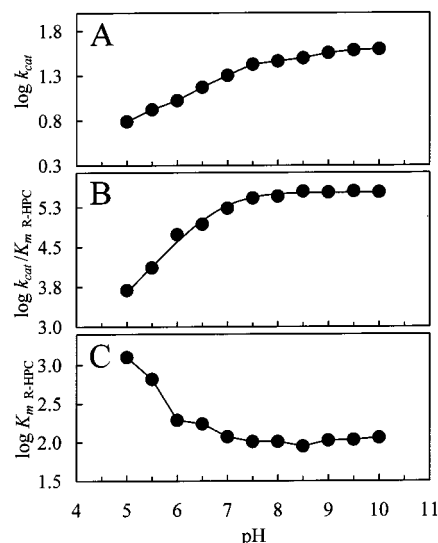
are shown in Table 4. Of the inhibitors intended to mimic a fraction of the R-HPC molecule (NaHSO$_4$, methanesulfonate, ethanesulfonate, and mercaptoethanesulfonate), all exhibited mixed inhibition with the exception of NaHSO$_4$ that was not inhibitory even up to 300 mM. These molecules demonstrated an exponentially increasing inhibitory trend (moving from methanesulfonate to mercaptoethanesulfonate) as the molecules began to more closely resemble substrate (Table 4).
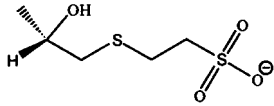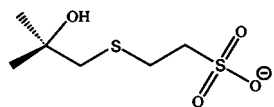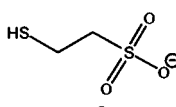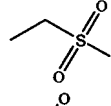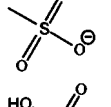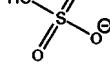
Time- and Concentration-Dependent Inactivation of rR-HPCDH with 2,3-Butanedione. As shown in Figure 4, 2,3-butanedione was found to be a time- and concentration-dependent inactivator of rR-HPCDH-catalyzed R-HPC oxidation. A plot of the log rate of inactivation (at each 2,3-butanedione concentration) versus log 2,3-butanedione concentration was fit using linear regression (slope 1.054, R^2 = 0.994) as described in Experimental Procedures (not shown). This indicated that rR-HPCDH inactivation observed in Figure 4 was pseudo first order with respect to 2,3-butanedione (*25*). The inset of Figure 4 is a plot of pseudo-first-order rate constants (*k*) versus 2,3-butanedione concentration and indicated that 2,3-butanedione did not saturate within the concentration range tested. The Figure 4 inset data were fit with linear regression (R^2 = 0.995) and yielded the true second-order rate constant of inactivation at 25 °C to be 0.031 M^{-1} s^{-1}.

Table 3: Summary of Amino Acid Substitutions Made to the Putative rR-HPCDH Catalytic Residues Using Site-Directed Mutagenesis[a]

amino acid	postulated catalytic role(s)[b]	substitution	V_{max} (units·mg^{-1})	K_m (μM R-HPC)	k_{cat} (s^{-1})	k_{cat}/K_m (M^{-1}·s^{-1})
		none	56.8 ± 0.5	102 ± 2	26.8	2.6 × 10^5
S142	H-bond donor to substrate/charge	S142A	0.47 ± 0.01^{ca}	836 ± 26	0.22	2.7 × 10^2
	stabilization of the transition state	S142C	no activity[d]			
Y155	general acid/base	Y155F	no activity[d]			
		Y155E	no activity[d]			
K159	lowers pK_a of Y155/coenzyme binding	K159A	no activity[d]			

[a] Abbreviations: R-HPC, 2-[(*R*)-2-hydroxypropylthio]ethanesulfonate. [b] Postulated catalytic roles are based on the trends thought to apply to most SDR enzymes. [c] Assays were performed in triplicate at 30 °C and pH 7.5 with 33 μg of S142A, variable R-HPC, and 10 mM NAD$^+$. [d] No activity was defined as no measurable increase in the absorbance at 340 nm (for NADH) in assays of standard length performed at 30 °C and pH 7.5 with 100 μg of mutant rR-HPCDH (25 times the standard assay amount), 2 mM R-HPC, and 20 mM NAD$^+$. One unit of enzyme activity was defined as 1 μmol of R-HPC oxidized per minute. k_{cat} and k_{cat}/K_m values were calculated using average V_{max} and K_m values as listed. V_{max} and K_m values are given as means ± standard deviations. All other values are given as means only.

Table 4: Rapid Equilibrium Inhibitors of the rR-HPCDH-Catalyzed Oxidation of 2-[(*R*)-2-Hydroxypropylthio]ethanesulfonate[a]

compd name	structure	type of inhibition	inhibition constants	
			K_{ic} (μM)	K_{iu} (μM)
S-HPC		competitive	156 ± 7	NA
M-HPC		competitive	406 ± 13	NA
mercaptoethanesulfonate		mixed	2250 ± 130	3620 ± 170
ethanesulfonate		mixed	26700 ± 800	38900 ± 2300
methanesulfonate		mixed	147800 ± 2600	122700 ± 5100
NaHSO$_4$		ND[b]	ND[b]	ND[b]

[a] Abbreviations: R-HPC, 2-[(*R*)-2-hydroxypropylthio]ethanesulfonate; S-HPC, 2-[(*S*)-2-hydroxypropylthio]ethanesulfonate; M-HPC, 2-(2-methyl-2-hydroxypropylthio)ethanesulfonate. Assays were performed in triplicate at 30 °C, pH 7.5, with variable amounts of R-HPC and 5 mM NAD$^+$. [b] Not determined; NaHSO$_4$ did not exhibit any inhibitory effects at concentrations up to 300 mM. All inhibition constants are listed as means ± standard deviations.

Substrate Protection Experiments with 2,3-Butanedione and Phenylglyoxal. With the knowledge that 2,3-butanedione was an inactivator, it was of interest to determine if the arginine residue(s) undergoing modification were in the vicinity of the active site. Two arginine modifiers were employed for this experiment because of their different van der Waals volumes and thus different potentials to be excluded by R-HPC. As shown in Figure 5, R-HPC protected against inactivation of rR-HPCDH by either 40 mM butanedione or 40 mM phenyglyoxal and demonstrated hyperbolic saturation. When 10 mM 2,3-butanedione was utilized, protection against inactivation by R-HPC was significantly greater at all concentrations tested (Figure 5). Na$_2$SO$_4$, which was used as a control to estimate salt effects on modification by 2,3-butanedione, exhibited approximately 11% protection at a concentration of 240 mM (Figure 5). However, protection afforded by Na$_2$SO$_4$ did not appear to saturate within the concentration range tested, and it was possible to fit data to a straight line with linear regression ($R^2 = 0.945$) (Figure

5). 2-Propanol afforded no measurable protection at concentrations up to 240 mM (Figure 5). The protection data from Figure 5 were fit to rectangular hyperbolas (using the standard form of the Michaelis−Menten equation) in order to calculate maximal percent protection (P_{max}) and the concentration of R-HPC giving half-maximal protection ($P_{1/2}$) for each condition tested (in ignorance to salt effects). R-HPC exhibited a P_{max} of 96% and a $P_{1/2}$ of 9 mM when 10 mM 2,3-butanedione was used in modification reactions. When modification reactions contained 40 mM 2,3-butanedione, the P_{max} and $P_{1/2}$ values were 92% and 31 mM, respectively. Similar results were obtained when S-HPC was used as the protectant, and in these experiments the simultaneous addition of 5 mM NAD$^+$ did not afford greater protection (data not shown). Modification reactions that contained 40 mM phenylglyoxal exhibited calculated P_{max} and $P_{1/2}$ values for R-HPC at 98% and 51 mM, respectively.

Amino Acid Analyses. Chemical modification studies are often plagued by lack of specificity, and nontargeted residues
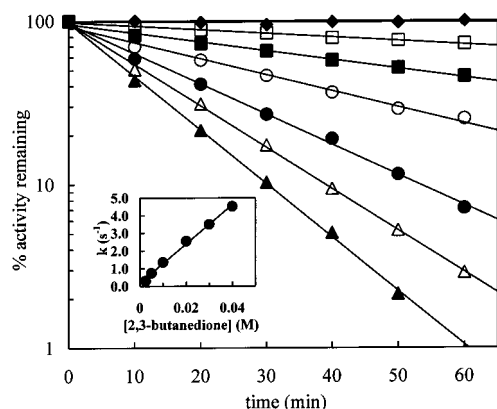
FIGURE 4: Time- and concentration-dependent inactivation of rR-HPCDH with 2,3-butanedione: (◆) no added 2,3-butanedione; (□) 2.5 mM, (■) 5 mM, (○) 10 mM, (●) 20 mM, (△) 30 mM, and (▲) 40 mM 2,3-butanedione. Inset: Pseudo-first-order rate constants of inactivation (determined for each 2,3-butanedione concentration) plotted against 2,3-butanedione concentration. The inset plot was fit with linear regression, and the slope was used to determine the true second-order rate constant of inactivation by 2,3-butanedione $(0.031 \ M^{-1} \cdot s^{-1})$.
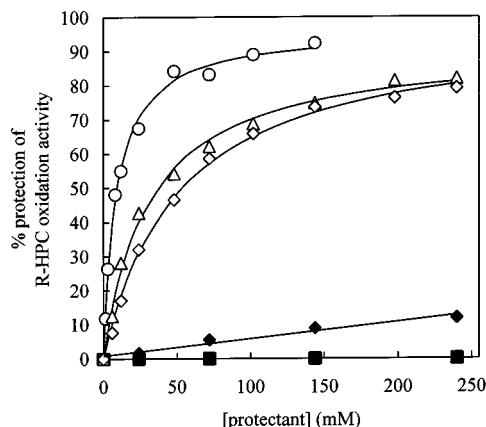

FIGURE 5: Abilities of 2-[(*R*)-2-hydroxypropylthio]ethanesulfonate (R-HPC), 2-propanol, and $NaHSO_4$ to protect against inactivation of rR-HPCDH by 2,3-butanedione and phenylglyoxal: (○) R-HPC as the protectant in assays containing 10 mM 2,3-butanedione, (△) R-HPC as the protectant in assays containing 40 mM 2,3-butanedione, (◇) R-HPC as the protectant in assays containing 40 mM phenylglyoxal, (◆) $NaHSO_4$ as the protectant in assays containing 40 mM 2,3-butanedione, and (■) 2-propanol as the protectant in assays containing 40 mM 2,3-butanedione. All assays utilizing R-HPC as the protectant were fit to a rectangular hyperbola described by the standard form of the Michaelis–Menten equation. Assays utilizing $NaHSO_4$ as a protectant were fit to a straight line using linear regression analysis. Data points represent the average of duplicate experiments.

are often destroyed at the expense of enzyme activity, which can cause one to misinterpret activity data (*30*). Fortunately, 2,3-butanedione has been called one of the most highly specific chemical modification reagents available (*26*) even in the wake of its potential to undergo undesirable photo-chemical reactions (*30, 31*). Despite its reputed specificity, it was of interest to both confirm arginine modification and ascertain the extent of destruction of other residues (if any) by 2,3-butanedione treatment of rR-HPCDH. This was accomplished using quantitative amino acid analysis of untreated enzyme and 2,3-butanedione-treated enzyme in the presence or absence of substrate (Figure 5). As shown in columns II, III, and IV, no significant changes (within their

standard deviations) occurred for Ser, Tyr, or Lys upon treatment with 2,3-butanedione in either the presence or absence of substrate. However, in the case of arginine, eight residues appear to be modified by treatment with 2,3-butanedione under the conditions tested [Table 5; Δ (II − III)]. By comparison, inclusion of S-HPC to enzyme treatments afforded an arguable measure of protection against modification, where only seven arginines seem to be modified [Table 5; Δ (III − IV)].

Activity of 2,3-Butanedione-Treated rR-HPCDH with Alternative Substrates. To investigate whether rR-HPCDH inactivation by 2,3-butanedione was simply the result of a destruction of its general catalytic ability, or an alteration of its unique ability to oxidize R-HPC, the relative activity of 2,3-butanedione-modified enzyme was compared with R-HPC and several secondary alcohols. As shown in Table 6, modified enzyme exhibited a greatly reduced activity toward R-HPC (28%). However, modified rR-HPCDH activity toward 2-propanol, (*R*)-2-pentanol, and (*R*)-2-heptanol was significantly greater (≥87%) (Table 6).

DISCUSSION

The R- and S-HPCDHs are homologous enzymes that are integral to the pathways of propylene and propylene oxide metabolism in the Gram-negative bacterium *Xanthobacter* strain Py2. On the basis of multiple sequence alignments, these two enzymes have been assigned to the short-chain dehydrogenase/reductase (SDR) superfamily, which is well represented in the scientific literature. Collectively, this body of literature supports a generalized catalytic mechanism that has been a useful starting point for the characterization of any newly identified SDR enzyme. Herein we report the heterologous expression of active R-HPC dehydrogenase and its subsequent characterization within the framework of this general mechanism. Additionally, the chemical modification and inhibition studies of the present work have begun to lay the foundation for a model of substrate binding that is expected to contribute to future studies aimed at understanding R-HPCDH enantioselectivity.

Product Inhibition. It has been established for some time that data from product inhibition experiments can give significant insight into an enzyme's kinetic mechanism. The kinetic mechanisms for several SDR enzymes have been determined and indicate that no single strategy can safely be assumed to envelop all members of the superfamily. In this regard compulsory-ordered (*32−34*), random-ordered (*35*), and a variant of the compulsory-ordered mechanism (Theorell−Chance) (*36*) have all been observed for SDR enzymes. As described here, the presence of either 2-KPC or NADH, during R-HPC oxidation, gave rise to three mixed and one competitive product inhibitions (Figure 2 and Table 1). Of these, it was only NADH and NAD$^+$ that were competitive, which indicated that only the coenzymes could productively bind to the free enzyme (Figure 2 and Table 1). In relation to the kinetic mechanisms observed for other SDR enzymes, noted above, these results were most consistent with the simple compulsory-ordered mechanism where coenzymes are the outer substrates (Scheme 2). The Theorell−Chance mechanism was excluded because 2-KPC would have been expected to be a competitive inhibitor with respect to R-HPC under the experimental conditions. Likewise,

Table 5: Quantitative Amino Acid Analysis of the rR-HPCDH[a]

| amino acid	I expected	II no additions	Δ (I − II)	III 2,3-BD	Δ (II − III)	IV 2,3-BD + S-HPC	Δ (III − IV)
Asx	25	24.30 ± 0.20	−0.70	25.40 ± 0.10	1.10	25.70 ± 0.20	0.30
Thr	17	17.00 ± 1.00	0.00	17.70 ± 0.02	0.70	18.10 ± 0.10	0.40
Glx	20	23.00 ± 2.00	3.00	22.30 ± 0.10	−0.70	22.70 ± 0.30	0.40
Pro	8	7.70 ± 0.50	−0.30	8.40 ± 0.30	−0.70	8.00 ± 1.00	−0.40
Gly	25	27.00 ± 2.00	2.00	26.30 ± 0.06	−0.70	26.40 ± 0.10	0.10
Ala	42	40.00 ± 4.00	−2.00	43.40 ± 0.10	3.40	43.50 ± 0.40	0.10
Cys	3	2.40 ± 0.50	−0.60	2.10 ± 0.20	−0.30	1.00 ± 1.00	−1.10
Val	29	26.00 ± 3.00	−3.00	29.00 ± 0.10	3.00	29.60 ± 0.30	0.60
Met	9	7.40 ± 0.50	−1.60	8.10 ± 0.10	0.70	5.40 ± 0.70	−2.70
Ile	13	12.30 ± 0.20	−0.70	13.02 ± 0.04	0.72	13.20 ± 0.10	−0.18
Leu	21	23.00 ± 0.40	2.00	24.00 ± 0.10	1.00	24.00 ± 0.20	0.00
Phe	6	6.50 ± 0.30	0.50	6.71 ± 0.02	−0.21	6.82 ± 0.02	−0.11
His	11	10.00 ± 1.00	−1.00	11.51 ± 0.03	1.51	11.40 ± 0.20	−0.11
Ser	16	18.00 ± 2.00	2.00	17.00 ± 0.10	−1.00	17.20 ± 0.20	0.20
Tyr	5	5.70 ± 0.50	0.70	5.60 ± 0.10	−0.10	5.40 ± 0.20	−0.20
Lys	5	6.00 ± 1.00	1.00	5.74 ± 0.02	−0.26	6.00 ± 0.10	−0.26
Arg	15	15.00 ± 0.10	0.00	7.30 ± 0.10	−7.70	8.30 ± 0.30	1.00

[a] Abbreviations: 2,3-BD, 2,3-butanedione; S-HPC, 2-[(S)-2-hydroxypropylthio]ethanesulfonate. Column I: expected number of amino acids based on the primary amino acid sequence of the rR-HPCDH. Column II: amino acid analysis of the unmodified rR-HPCDH. Column III: amino acid analysis of the rR-HPCDH incubated with 40 mM 2,3-butanedione for 60 min at 30 °C. Column IV: amino acid analysis of the rR-HPCDH treated as in column III but with the addition of S-HPC (150 mM). Intervening columns indicate the changes between the values in selected columns. All amino acid analyses were performed in triplicate. Numerical values represent the average number of moles of amino acid per mole of protein ± standard deviations.

Table 6: Relative Activity of the rR-HPCDH with Selected Secondary Alcohols Following Chemical Modification with 2,3-Butanedione[a]

substrate	[substrate][b] (mM)	relative activity (%) after modification	Δ relative activity (%) vs R-HPC
R-HPC	0.100	28.1 ± 0.7	0
2-propanol	650	97.2 ± 2.9	+69.1
(R)-2-pentanol	20	94.8 ± 1.3	+66.7
(R)-2-heptanol	2.5	87.2 ± 3.6	+59.1

[a] Abbreviation: R-HPC, 2-[(R)-2-hydroxypropylthio]ethanesulfonate. Chemical modification was carried out with 40 mM 2,3-butanedione and 80 μM rR-HPCDH at 25 °C for 45 min. [b] All substrate concentrations were equal to or less than the concentration producing half-maximal rates. Values represent the average of five experiments ± standard deviations.

Scheme 2
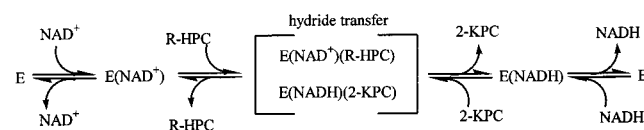
variants of the random-ordered mechanism were excluded because of lack of agreement with the observed pattern of product inhibition.

The underlying reasons as to why compulsory-ordered enzyme mechanisms are observed are thought to lie in protein structural changes. The induced fit hypothesis for enzymes following a compulsory-ordered mechanism suggests that binding of the first substrate initiates structural change that facilitates binding of the second substrate. The three-dimensional structures for several SDR enzymes have been determined in both the free and substrate-bound forms. In general, these studies indicate that structural rearrangements occur upon substrate binding, and because so, conformational changes are now thought to be a common feature of all SDR enzymes (37). These changes are perhaps best exemplified

by considering two enzymes that follow a compulsory-ordered mechanism as in Scheme 2, the *Drosophila* alcohol dehydrogenase and the human 7α-hydroxysteroid dehydrogenase. For both enzymes, crystallographic analyses have revealed that the transition from the free enzyme to the enzyme·NAD$^+$ binary complex results in significant conformational changes to the C-terminal substrate binding loop, a region involved in binding a SDR enzyme unique substrate (37, 38). While real evidence for R-HPCDH structural rearrangements upon NAD$^+$ binding must await completion of structural studies in progress, the possibility of structural changes upon NAD$^+$ binding is nevertheless implied by its kinetic mechanism.

Site-Directed Mutagenesis. It is commonly accepted that the highly conserved serine, tyrosine, and lysine residues observed in multiple sequence alignments of SDR enzymes constitute a catalytic triad, whose functions are part of a general mechanism (6). In this mechanism, the serine plays a role in substrate binding by making a hydrogen bond to the substrate oxygen and a role in catalysis by contributing to charge stabilization of the anionic transition state. The tyrosine is the catalytic acid/base that deprotonates the alcohol substrate in the forward direction or protonates the ketone in the reverse reaction, concomitant with hydride transfer. Last, the conserved lysine is thought to lower the pK_a of the tyrosine and bind coenzyme via an interaction with the 2'- and 3'-hydroxyls of the nicotinamide ribose.

The previous catalytic triad assignments for R-HPCDH (S142, Y155, and K159) made on the basis of sequence alignments (4) are supported by the loss of activity observed for mutant proteins with amino acid substitutions at these positions (Table 3). The inactivity of the Y155F mutant is consistent with the elimination of the essential acid/base, and the inactivity of the Y155E mutant shows that an alternate ionizable residue is unable to substitute in the reaction (Table 3). In the case of the K159A mutant, no activity was observed over the range of pH values tested (5−11). The lack of

activity at the highest pH, where an unperturbed tyrosine should be able to function in the role of general base, supports a dual role for K159 in lowering the pK_a of tyrosine and in coenzyme binding.

The low activity observed for the S142A mutant indicates that this serine is not obligatory for R-HPC oxidation activity but clearly is a contributor to both R-HPC binding and oxidation. The nonobligatory role of this residue has been demonstrated for a small number of SDR enzymes that lack a serine at this position in the wild-type form. The unexpected absence of activity for the S142C mutant initially appeared to be contradictory with the proposed role of S142. A thiol proton, after all, might partially substitute for an alcoholic proton as a mere hydrogen bond donor to R-HPC. The inhibitory nature of the cysteine at position 142 was therefore rationalized by considering the unique properties of the side-chain thiol. A comparison of the van der Waals radii of oxygen (∼1.4 Å) and sulfur (∼1.8 Å) atoms and the pK_as for an unperturbed cysteine thiol (p$K_a \cong 8$) and serine alcohol (p$K_a \geq 14$) indicated clear distinctions. These distinctions hinted that S142C inactivity may be caused by a combination of subtle steric effects and formation of a partially deprotonated cysteine. In the case of cysteine deprotonation, an extra partial negative charge in the active site could severely alter substrate binding and proper functioning (i.e., pK_a) of the catalytic acid/base. It is also possible, although unlikely based on our characterization of the mutant enzyme, that the lack of activity is a result of disulfide bond formation or another structural phenomenon unrelated to catalysis but resulting from this amino acid substitution.

pH Dependence of Kinetic Parameters. Analysis of the pH-dependent variation of kinetic parameters for an enzyme can contribute to a greater understanding of its chemical mechanism by helping to discover, and in some cases identify, groups important for catalysis. However, among other things, substrate ionization, a pH-induced change in kinetic mechanism, or pH-induced change in protein structure can complicate such studies, and so pH data must be interpreted with great caution. With respect to interpretation of our data, substrate ionization was not a concern, owing to the absence of titratable groups on R-HPC over the pH range studied and use of a saturating concentration of NAD$^+$ at each pH. A pH-induced change in kinetic mechanism was also considered, even though at least one SDR enzyme in the literature demonstrated a compulsory-ordered mechanism (with coenzymes as the outer substrates) across the entire pH range (6−10) of the study (*32*). On a final note, pH-induced instability and/or change in protein structure did not appear to be a concern for R-HPCDH, because the rates of NAD$^+$ reduction (at all pHs) appeared to be linear within the assay time frames (<25 s).

log k_{cat} data for R-HPC oxidation were plotted against pH to visualize its effect on the turnover number for R-HPC oxidation (Figure 3A). Variations in slope for this type of plot reflect a change in the ionization state of groups on the enzyme·substrate complex or, in the present case, the R-HPCDH ternary complex, where both NAD$^+$ and R-HPC are bound. However, the pH dependence of k_{cat} can also be thought of as a measure of the pH dependence of the rate-determining step in the breakdown of the ternary complex to free enzyme and free products. For the R-HPCDH, breakdown of the enzyme·NAD$^+$·R-HPC ternary complex

presumably occurs through the steps shown in Scheme 2, where hydride transfer is followed by two distinct product release steps. As shown in Figure 3A, no significant changes in slope were observed, although a steady increase in log k_{cat} was seen as the pH was increased. Given the key role that deprotonated Y155 is thought to play in initiating hydride transfer, the lack of significant slope changes (ionizations) in Figure 3A may suggest that hydride transfer is only partially rate-determining. In reality, this observation might be preliminary evidence that the primary rate-determining step is product release (NADH?) as determined for other SDR enzymes, such as the *Drosophilia lebanonensis* alcohol dehydrogenase, that follow a compulsory-ordered kinetic mechanism (*32*). For such enzymes, the conformational change/isomerization associated with NAD$^+$ binding must be reversed for NADH to depart, and it is this step that appears to be rate-determining. With this consideration in mind, the increase in k_{cat} for R-HPC oxidation at higher pHs could conceivably reflect the pH dependence of an enzyme isomerization step that is necessary for NADH release.

Variations in slope for a log k_{cat}/K_{mR-HPC} plot (in the absence of substrate ionization) reflect changes in the ionization state of groups on the free enzyme necessary for catalysis (*25*). Typically, an enzyme requiring that a particular group be deprotonated for catalysis will exhibit a decrease in the k_{cat}/K_m value with decreasing pH. The slope of this decrease reflects the number of ionizations in the free enzyme, where a slope of 1 would be expected if protonation of a single group on the free enzyme decreases the value of k_{cat}/K_m and, likewise, a slope of 2 if two ionizable groups are involved (*39*). When the experimental data points between pH 5.0 and pH 6.0 (inclusive) of Figure 3B were fit to a straight line, a slope of 1.05 was observed. However, a similar analysis of Figure 3B data between pH 5.0 and pH 7.0 (inclusive) yielded a slope of 0.78.

Unique situations have been described in the literature for slopes less than 1 (*39*), and while these possibilities cannot be completely ruled out without further experimentation beyond the scope of this work, we proposed the slope of Figure 3B to be approximately 1. With NAD$^+$ saturating, this suggested that a single ionizable residue on the enzyme· NAD$^+$ binary complex was responsible for the change in slope of Figure 3B and that deprotonation of this residue was required for efficient catalysis. As noted in the Results, the pK_a of the single ionizing residue is 6.9. By comparison to the pH studies of other SDR enzymes, this ionization likely represents the tyrosine general acid/base (Y155) of the rR-HPCDH catalytic triad. The acid dissociation constant of the catalytic tyrosine has been reported for a few SDR enzymes, most notably the *Drosaphila melanogaster* alcohol dehydrogenase with a pK_a of 7.6 (*40*).

The log K_{mR-HPC} vs pH plots were intended to visualize the effect of pH on the relative affinity of the enzyme·NAD$^+$ binary complex for R-HPC (Figure 3C). The K_m for R-HPC decreased greater than 12-fold over the pH from 5.0 to 8.5, in a manner that paralleled the leveling off of the log k_{cat}/K_m value in Figure 3B. These data suggest a dual role for Y155 in alcohol binding (K_m effect) and deprotonation (k_{cat}/K_m effect). Y155, with a pK_a of 6.9, would be fully deprotonated at a pH of 8−8.5 and, concomitantly, would be expected to have a maximum attraction to the alcohol of R-HPC at this and higher pH values.

Aside from the alcohol, the negatively charged sulfonate of R-HPC stands out as a potential binding point, and this group has been proposed to interact with a positively charged residue (*18*). The amino acids with positively charged side chains include histidine, lysine, and arginine, and any of them could conceivably interact with the anionic sulfonate of R-HPC. As shown in Table 2 and Figure 3C, the K_m for R-HPC remains unchanged (within errors) at higher pHs. This result does not seem to support either histidine or lysine as candidates to interact with the sulfonate. If either interacted with the sulfonate, and indeed interaction with the sulfonate is significant to binding, the K_m would be expected to rise abruptly as histidine (unperturbed $pK_a = 6$) is completely deprotonated or as lysine begins to be deprotonated (unperturbed $pK_a = 10.5$) at high pHs. Arginine, on the other hand, has a side-chain guanidino group with an unperturbed pK_a of 12.5 that would allow it to be completely protonated/positively charged over the entire pH range of this study. This would enable one or more arginines to bind the R-HPC sulfonate efficiently at high pHs. This presumption is supported by the literature that has emphasized arginine as a key player in the binding of anionic substrates (*41*, *42*).

Chemical Modification. As mentioned above, the pH independence of K_{mR-HPC} at high pHs (Figure 3C) suggested possible involvement of a high pK_a residue(s), possibly one or more arginines, in substrate binding. A functional role for arginine in R-HPCDH activity was also suggested by the time- and concentration-dependent inactivation of R-HPC oxidation activity by the arginine-specific reagents 2,3-butanedione and phenylglyoxal and the fact that both inactivation processes could be prevented by R-HPC (Figure 5). The results from amino acid analysis suggested that one arginine was protected against modification by S-HPC (Table 5). Collectively, these experiments indicated that arginines are important for activity and that one arginine in the active site is made inaccessible to reagent when S-HPC is present. The data in Table 6, where enzyme is shown to be inactivated toward R-HPC oxidation but not the oxidation of non-sulfonic acid alcohols, suggest either an indirect role in active site formation or a direct role in R-HPC binding. At present we favor the latter or that an arginine, which normally serves to complex the sulfonate of R-HPC, is sterically prevented from doing so upon chemical modification. In contrast, other alcohols, not requiring interaction with this arginine or binding at the same site, are not sterically impeded by modification and as a result can bind and turnover normally.

Activity with a Substrate Analogue. The kinetic parameters for the oxidation of the primary alcohol 2-HEC, an analogue of R-HPC that lacked the terminal methyl group, were drastically different than those determined for R-HPC. In particular, the values of k_{cat} and K_m were approximately 2 orders of magnitude lower and 7.5-fold higher, respectively, than the values obtained when R-HPC was the substrate. The drastically reduced k_{cat} for 2-HEC oxidation suggested the possibility that a change in the rate-determining step occurs with this substrate. If, as hypothesized above, the RDS for R-HPC oxidation is NADH release, then it is feasible that, for 2-HEC oxidation, the hydride-transfer step may be rate-determining. In corroboration of this idea, it would be of interest to determine the magnitude of the isotope effect for the deuterated form of this substrate and the pH dependence of the kinetic parameters for its oxidation. Last, the signifi-

cantly higher K_m obtained with 2-HEC appeared to highlight the contribution of the terminal methyl group to substrate binding.

Rapid Equilibrium Inhibition. The determination of the inhibition constants for the compounds in Table 4 has helped to define the R-HPCDH active site and define the relative contribution of groups on the R-HPC mercaptoethanesulfonate "tail" to binding. As shown in Table 4, S-HPC was found to be a competitive inhibitor with a K_{ic} value (156 ± 7 μM) close to the K_m for R-HPC (105 ± 2 μM). This was intriguing, because it suggested that both HPC enantiomers could bind with a similar affinity to R-HPCDH, a finding that argued against any underlying mechanism of enantiodiscrimination. Instead, the poor rate of S-HPC turnover, previously observed for R-HPCDH, is most likely due to the position of the removable hydride of S-HPC in relation to NAD$^+$. M-HPC is a tertiary alcohol that was also found to be a competitive inhibitor (Table 4). Given that M-HPC lacks an abstractable hydride and has a reasonable affinity for R-HPCDH, it might prove useful in binding studies and crystallographic characterization requiring a nonturnover R-HPC analogue.

As shown in Table 4, the addition of a single methyl group to methanesulfonate increased the recognition by R-HPCDH 5-fold. Furthermore, addition of a thiol to ethanesulfonate increased recognition an additional 10-fold. This contribution, however, is difficult to extrapolate to any added affinity afforded by the R-HPC thioether, because of the possibility that this compound is binding directly to Y155 via the thiol in a manner different than that of the R-HPC tail. In fact, the mixed nature of these three inhibitors, in relation to R-HPC, indicated they could bind to multiple forms of the enzyme. If these inhibitors are truly binding in a manner analogous to that of the mercaptoethanesulfonate portion of R-HPC, then at the very least, these inhibiton data provide insight to the binding contribution of the mercaptoethanesulfonate methylenes of R-HPC.

Summary and Concluding Remarks. The results presented in this paper have developed the prerequisite foundation for additional studies of the enantioselective mechanism of the rR-HPCDH and its partner enzyme (S-HPCDH). The product inhibition of this work supports a compulsory-ordered ternary mechanism, with NAD$^+$ as the first substrate to bind and, by extrapolation, NADH as the last product to leave. Site-directed mutagenesis data have elucidated the obligatory and nonobligatory roles of Y155 and K159 and of S142 to activity, respectively, and have provided evidence for prior assumptions based purely on sequence alignments. Investigation of the dependence of the kinetic parameters on pH has allowed the pK_a of a single catalytically important residue on the rR-HPCDH·NAD$^+$ binary complex to be determined, and by analogy to other SDR enzymes, this residue is thought to be Y155, i.e., the acid/base of the catalytic triad. The use of arginine-specific modifiers combined with substrate protection experiments and amino acid analysis has suggested that one or more active site arginines are essential for rR-HPCDH activity. By investigating the activity of the modified enzyme with alternate substrates, it was determined that the putative arginine(s) are very important to the turnover of R-HPC and less so to the oxidation of non-sulfonic acid alcohols. These data provided additional support to the role of one or more arginines in R-HPC binding. In its entirety,

this study is the first of its kind for an SDR enzyme having a partner that catalyzes the same reaction but with an opposite stereospecificity. In a broader biochemical context, this work has expanded the limited mechanistic knowledge of enzymes essential to bacterial alkene and epoxide metabolism.

ACKNOWLEDGMENT

REFERENCES

1. Schmid, A., Dordick, J. S., Haner, B., Kiener, A., Wubbolts, M., and Witholt, B. (2001) *Nature 409*, 258−268.
2. Sotolongo, V., Johnson, D. V., Wahnon, D., and Wainer, I. W. (1999) *Chirality 11*, 39−45.
3. Allen, J. R., Clark, D. D., Krum, J. G., and Ensign, S. A. (1999) *Proc. Natl. Acad. Sci. U.S.A. 96*, 8432−8437.
4. Allen, J. R., and Ensign, S. A. (1999) *Biochemistry 38*, 247−256.
5. Krozowski, Z. (1994) *J. Steroid Biochem. Mol. Biol. 51*, 125−130.
6. Jornvall, H., Persson, B., Krook, M., Atrian, S., Gonzalez-Duarte, R., Jeffery, J., and Ghosh, D. (1995) *Biochemistry 34*, 6003−6013.
7. Oppermann, U. C. T., Filling, C., and Jornvall, H. (2001) *Chem.-Biol. Interact. 130−132*, 699−705.
8. Smilda, T., Reinders, P., and Beintema, J. J. (1998) *Biochem. Genet. 36*, 37−48.
9. Nakajima, K., Yamashita, A., Akama, H., Nakatsu, T., Kato, H., Hashimoto, T., Oda, J.-i., and Yamada, Y. (1998) *Proc. Natl. Acad. Sci. U.S.A. 95*, 4876−4881.
10. Allard, S. T., Giraud, M. F., Whitefield, C., Graninger, M., Messner, P., and Naismith, J. H. (2001) *J. Mol. Biol. 307*, 283−295.
11. Benach, J., Atrian, S., Gonzalez-Duarte, R., and Landenstein, R. (1998) *J. Mol. Biol. 282*, 383−399.
12. Otagiri, M., Kurisu, G., Ui, S., Takusagawa, Y., Ohkuma, M., Kudo, T., and Kusunoki, M. (2001) *J. Biochem. (Tokyo) 129*, 205−208.
13. Yamamoto, K., Kurisu, G., Kunsunoki, M., Tabata, S., Urabe, I., and Osaki, S. (2001) *J. Biochem. (Tokyo) 129*, 303−312.
14. Rosano, C., Bisso, A., Izzo, G., Tonetti, M., Sturla, L., De Flora, A., and Bolognesi, M. (2000) *J. Mol. Biol. 303*, 77−91.
15. Mulichak, A. M., Theisen, M. J., Essigmann, B., Benning, C., and Garavito, R. M. (1999) *Proc. Natl. Acad. Sci. U.S.A. 96*, 13097−13102.
16. Baldock, C., Rafferty, J. B., Stuitje, A. R., Slabas, A. R., and Rice, D. W. (1998) *J. Mol. Biol. 284*, 1529−1546.
17. Nakajima, K., Hashimoto, T., and Yamada, Y. (1993) *Proc. Natl. Acad. Sci. U.S.A. 90*, 9591−9595.
18. Ensign, S. A. (2001) *Biochemistry 40*, 5845−5853.
19. Clark, D. D., Allen, J. R., and Ensign, S. A. (2000) *Biochemistry 39*, 1294−1304.
20. Krum, J. G., and Ensign, S. A. (2000) *J. Bacteriol. 182*, 2629−2634.
21. Allen, J. R., and Ensign, S. A. (1997) *J. Biol. Chem. 272*, 32121−32128.
22. Chromy, V., Fischer, J., and Kulhanek, V. (1974) *Clin. Chem. 20*, 1360−1363.
23. Laemmli, U. K. (1970) *Nature 227*, 680−685.
24. Cleland, W. W. (1979) *Methods Enzymol. 63*, 103−138.
25. Cornish-Bowden, A. (1995) *Fundamentals of enzyme kinetics*, Portland Press Ltd., London, U.K.
26. Epperly, B. R., and Dekker, E. E. (1989) *J. Biol. Chem. 264*, 18296−18301.
27. Hockney, R. C. (1994) *Trends Biotechnol. 12*, 456−463.
28. Copeland, R. A. (2000) *Enzymes: A practical introduction to structure, mechanism, and data analysis*, Wiley-VCH, Inc., New York.
29. Segel, I. H. (1993) *Enzyme kinetics. Behavior and analysis of rapid-equilibrium and steady-state enzyme systems*, John Wiley and Sons, Inc., New York.
30. Eyzaguirre, J. (1996) *Biol. Res. 29*, 1−11.
31. Makinen, K. K., Makinen, P.-L., Wilkes, S. H., Bayliss, M. E., and Prescott, J. M. (1982) *J. Biol. Chem. 257*, 1765−1772.
32. Brendskag, M. K., McKinley-Mckee, J. S., and Winberg, J.-O. (1999) *Biochim. Biophys. Acta 1431*, 74−86.
33. Winberg, J.-O., and McKinley-Mckee, J. S. (1994) *Biochem. J. 301*, 901−909.
34. Luba, J., Nare, B., Liang, P. H., Anderson, K. S., Beverley, S. M., and Hardy, L. W. (1998) *Biochemistry 37*, 4093−4104.
35. Menon, S., Stahl, M., Kumar, R., Guang-Yi, X., and Sullivan, F. (1999) *J. Biol. Chem. 274*, 26743−26750.
36. Hallis, T. M., Lei, Y., Que, N. L., and Lui, H. (1998) *Biochemistry 37*, 4935−4945.
37. Tanaka, N., Nonaka, T., Tanabe, T., Yoshimoto, T., Tsuru, D., and Mitsui, Y. (1996) *Biochemistry 35*, 7715−7730.
38. Benach, J., Gonzalez-Duarte, R., and Ladenstein, R. (1999) *J. Mol. Biol. 289*, 335−355.
39. Cleland, W. W. (1986) in *Investigations of rates and mechanisms of reactions* (Bernasconi, C. F., Ed.) pp 792−870, John Wiley and Sons, Inc., New York.
40. McKinley-Mckee, J. S., Winberg, J., and Pettersson, G. (1991) *Biochem. Int. 25*, 879−885.
41. Riordan, J. F. (1979) *Mol. Cell. Biochem. 26*, 71−92.
42. Riordan, J. F., McElvany, K. D., and Borders, C. L. J. (1977) *Science 195*, 884−886.